

## Original Article

# Multivariate analysis of the volumetric capnograph for PaCO<sub>2</sub> estimation

Slava M Belenkiy<sup>1</sup>, William L Baker<sup>1</sup>, Andriy I Batchinsky<sup>1,2</sup>, Sumit Mittal<sup>1</sup>, Taylor Watkins<sup>1</sup>, Jose Salinas<sup>1</sup>, Leopoldo C Cancio<sup>1,3</sup>

<sup>1</sup>U.S. Army Institute of Surgical Research, USA; <sup>2</sup>University of Texas Medical Branch, Galveston, TX, USA;

<sup>3</sup>University of Texas Health Science Center at San Antonio, TX, USA

Received July 9, 2015; Accepted September 24, 2015; Epub October 12, 2015; Published October 15, 2015

**Abstract:** Purpose: End-tidal CO<sub>2</sub> (eTCO<sub>2</sub>) can be used to estimate the arterial CO<sub>2</sub> (PaCO<sub>2</sub>) under steady-state conditions, but that relationship deteriorates during hemodynamic or respiratory instability. We developed a multivariate method to improve our ability to estimate the PaCO<sub>2</sub>, by using additional information contained in the volumetric capnograph (Vcap) waveform. We tested this approach using data from a porcine model of chest trauma/hemorrhage. Methods: This experiment consisted of 3 stages: pre-injury, injury/resuscitation, and post-injury. In stage I, anesthetized pigs (n=26) underwent ventilator maneuvers (tidal volume and respiratory rate) to induce hypo- or hyper-ventilation. In stage II, pigs underwent either (A) unilateral pulmonary contusion, hemorrhage, and resuscitation (n=13); or (B) bilateral pulmonary contusion (n=13) followed by 30 min of monitoring. In stage III, the ventilator maneuvers were repeated. The following Vcap features were measured: eTCO<sub>2</sub>, phase 2 slope (p2m), phase 3 slope (p3m), and inter-breath interval. The data were fit to 2 models: (1) multivariate linear regression and (2) a machine-learning model (M5P). Results: 1750 10-breath sets were analyzed. Univariate models employing eTCO<sub>2</sub> alone were adequate during stages I and III. During stage II, mean error for the linear model was -8.44 mmHg (R<sup>2</sup>=0.14, P<0.001) and for M5P it was -5.98 mmHg (R<sup>2</sup>=0.13, P<0.01). By adding Vcap features, all models exhibited improvement. In stage II, the mean error of the linear model improved to -4.64 mmHg (R<sup>2</sup>=0.11, P<0.01), and that of the M5P model improved to -1.62 mmHg (R<sup>2</sup>=0.25, P<0.01). Conclusions: By incorporating Vcap waveform features, multivariate methods modestly improved PaCO<sub>2</sub> estimation, especially during periods of hemodynamic and respiratory instability. Further work would be needed to produce a clinically useful CO<sub>2</sub> monitoring system under these challenging conditions.

**Keywords:** End-tidal carbon dioxide, arterial carbon dioxide, capnography, pulmonary contusion, hemorrhage, machine learning

## Introduction

Capnography is the measurement and display of the partial pressure of carbon dioxide in the exhaled breath. Capnographic monitoring is increasingly recognized as an important tool in critical care and emergency medicine, because it helps achieve the 4 immediate priorities of resuscitation: airway, breathing, circulation, and disability [1]. For *airway* management, it confirms endotracheal tube placement and alerts the provider if the tube becomes dislodged. For *breathing* management, end-tidal carbon dioxide (eTCO<sub>2</sub>), under hemodynamically stable conditions, correlates with arterial carbon dioxide (PaCO<sub>2</sub>) and provides a non-inva-

sive estimate of ventilation adequacy. For *circulation* management, onset of cardiac arrest and hemorrhagic shock are quickly reflected in decreases in eTCO<sub>2</sub> [2]. Conversely, eTCO<sub>2</sub> rises during adequate chest compressions [3]. For *disability* management, capnography is indicated for the treatment of intubated patients with head injury, since cerebral blood flow is adversely affected by hypocapnia [4]. Because of these and similar considerations, capnography is recommended by the American Society of Anesthesiologists [5], the Advanced Trauma Life Support course [6] the Advanced Cardiovascular Life Support course [3], and the Brain Trauma Foundation's prehospital guidelines [7].

In several of the above applications, a close relationship between the  $e\text{TCO}_2$  and  $\text{PaCO}_2$  is assumed. However, rapidly changing hemodynamic or respiratory conditions alter the relationship between  $e\text{TCO}_2$  and  $\text{PaCO}_2$ . For example, an increase in alveolar dead space due to deterioration of pulmonary function increases the divergence between  $e\text{TCO}_2$  and  $\text{PaCO}_2$ . In patients with healthy lungs, this divergence is small, justifying the use of  $e\text{TCO}_2$  as a surrogate for  $\text{PaCO}_2$ . In patients with diseased lungs, the baseline  $e\text{TCO}_2$ -to- $\text{PaCO}_2$  difference must be measured, allowing subsequent estimates of the  $\text{PaCO}_2$  to be more accurately estimated [8]. But if the dead space changes with worsening (or improving) disease, then  $e\text{TCO}_2$  becomes less reliable as a  $\text{PaCO}_2$  surrogate. Decreased perfusion of the lung, e.g. in cardiogenic shock or hemorrhagic shock, also increases the  $e\text{TCO}_2$ -to- $\text{PaCO}_2$  difference and interferes with the utility of the  $e\text{TCO}_2$  as a surrogate for  $\text{PaCO}_2$  [9].

In a porcine model of chest trauma and hemorrhage, we recently confirmed the close correlation between  $e\text{TCO}_2$  and  $\text{PaCO}_2$  across a wide range of minute-ventilation levels, both before injury and after resuscitation. However, the  $e\text{TCO}_2$ -to- $\text{PaCO}_2$  relationship deteriorated significantly immediately after injury and during hemorrhagic shock [10].

Because of these limitations and in order to improve our ability to predict  $\text{PaCO}_2$  in unstable patients, we reexamined the information content of the exhaled  $\text{CO}_2$  waveform. We employed the volumetric capnograph (Vcap), which is the result of plotting the exhaled  $\text{CO}_2$  against the exhaled breath volume on a breath-by-breath basis. This differs from the usual capnograph, in which exhaled  $\text{CO}_2$  is displayed as a function of time. Certain features of the Vcap waveform correlate with ventilation-perfusion (V/Q) dispersion, a global index of V/Q mismatch [11]. Previously, a multivariate approach was applied to data obtained from Vcap waveform features, to predict the presence of pulmonary embolism [12]. The purpose of the current study was to develop and evaluate an improved algorithm for estimating  $\text{PaCO}_2$  using readily available features of the volumetric capnograph. We hypothesized that multivariate assessment of these features could improve our ability to estimate  $\text{PaCO}_2$  noninvasively, despite rapidly changing pulmonary and hemodynamic conditions.

### Materials and methods

This study was approved by the U.S. Army Institute of Surgical Research, Institutional Animal Care and Use Committee. It was conducted in compliance with the Animal Welfare Act and the implementing Animal Welfare Regulations and in accordance with the principles of the *Guide for the Care and Use of Laboratory Animals*.

#### Animal preparation

This study consisted of analysis of data from previously reported animal experiments [10]. Briefly, 26 female Yorkshire pigs (Midwest Research Swine, Gibbon, MN) weighing 30 to 45 kg were fasted overnight and premedicated with glycopyrolate. Inhaled isoflurane (0.5-3.0 vol%) was used to induce anesthesia. Animals were intubated, and midazolam (25 mg/h), ketamine (250  $\mu\text{g}/\text{kg}/\text{min}$ ), and propofol (150  $\mu\text{g}/\text{kg}/\text{min}$ ) were administered for total intravenous anesthesia (TIVA). A tracheostomy was performed. The femoral arteries, femoral veins, and right external jugular vein were catheterized. The animals were then placed in the sternal recumbent position. They were mechanically ventilated using a Dräger EVITA XL ventilator (Dräger Medical, Telford, Pa), initially with a tidal volume (TV) of 10 mL/kg and a respiratory rate (RR) of 12 breaths/min. The fraction of inspired oxygen ( $\text{FiO}_2$ ) and the positive end-expiratory pressure were set to 21% and 5 mmHg, respectively. A mainstream Vcap monitor ( $\text{CO}_2\text{SMO}$ ; Philips Respironics, Amsterdam, Netherlands) was connected to the endotracheal tube. A pulse oximeter (Oxisensor II 1-20; Covidien; Nellcor, Mansfield, Mass) was placed on the tail to measure peripheral saturation of oxygen ( $\text{SpO}_2$ ). Blood gases were measured using a point-of-care device (iSTAT, Abbott Laboratories, Abbott Park, IL). The  $\text{FiO}_2$  of the ventilator was adjusted to maintain a minimum  $\text{SpO}_2$  of 90%.

#### Experimental protocol

Both experiments consisted of 3 stages. On day 1, the animals were surgically prepared as described above, and underwent a sequence of respiratory maneuvers (*stage I*; see below). The animals were then rested overnight in the animal ICU. The next day, they were placed in the dorsal recumbent position and underwent *stage II*. This consisted of either unilateral

## Volumetric capnography

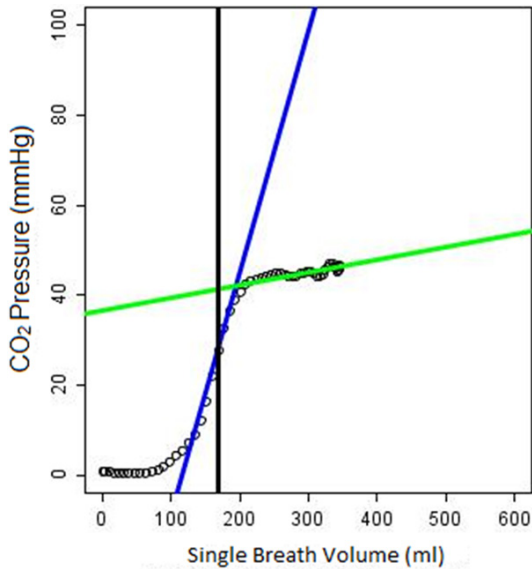


**Figure 1.** Example of Vcap waveform. Blue line: phase 2 slope (p2m), phase 2 intercept (p2i), Green line: phase 3 slope (p3m), phase 3 intercept (p3i), Black line: Airway Dead Space (in mL).

(right-sided) (Group A, n=13) or bilateral pulmonary contusions (Group B, n=13) [13]. Those animals in Group A then underwent hemorrhage (12 mL/kg over 10 min), a shock period of 30 min, and rapid resuscitation with lactated Ringer's (3 times the shed volume) and shed blood. No respiratory maneuvers were performed during stage II. After resuscitation, the animals were returned to the sternal recumbent position and the same respiratory maneuvers as in stage I were performed again (stage III). Upon completion of stage III, the animals were euthanized with high-dose sodium pentobarbital solution (Fatal-Plus, Dearborn, MI).

For the respiratory maneuvers in stages I and III, a sequence of ventilator changes were performed by varying the RR or TV to induce hypoventilation or hyperventilation. After baseline measurements, each animal was randomized into 1 of 4 groups to determine the sequence by which the respiratory maneuvers would be done. Before respiratory maneuvers and after ensuring adequate analgesia, animals were administered a vecuronium bolus (1 mg/kg) to ensure the absence of spontaneous respiration. Blood gas analysis was performed at 5 and 7 min after each respiratory maneuver; PaCO<sub>2</sub> values were recorded and the results were averaged.

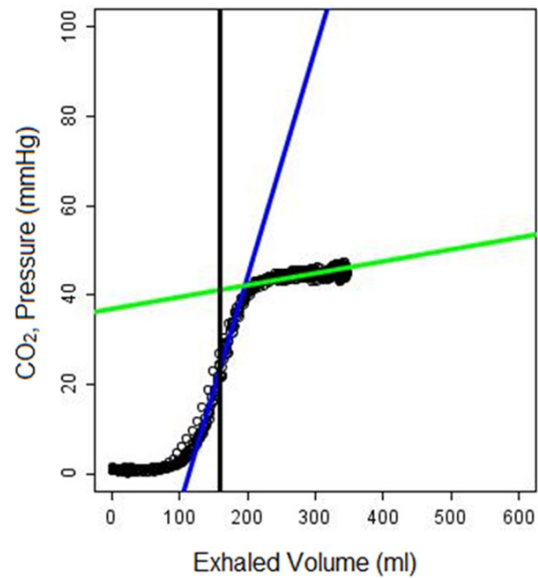


**Figure 2.** Composite Vcap curve consisting of ten overlaid breaths.

### Capnographic analysis

Ventilator settings and continuous capnography waveforms were recorded from the CO<sub>2</sub> SMO device to a computer by custom-built software, the Integrated Data Exchange and Archival (IDEA) system.

A Java-based computer program was written to analyze the ventilator waveforms and to segment each breath. The Vcap curves were obtained by plotting the partial pressure of CO<sub>2</sub> as a function of the volume of exhaled breath. The curves were then parameterized as described previously by Fletcher [14, 15]. The Vcap curve is characterized by three phases (**Figure 1**). Phase 1 is an initial flat phase, low in CO<sub>2</sub>, which corresponds to exhalation of air from the anatomical dead space that has not undergone gas exchange at the alveoli. Phase 2 is characterized by a rapid rise in CO<sub>2</sub> due to mixing of air from the dead space and the alveoli. Phase 3 consists of alveolar gas and is characterized by a plateau, with a slight incline, that terminates in the CO<sub>2</sub> partial pressure recognized as eTCO<sub>2</sub>.

Slopes and intercepts for each phase were determined and named as follows: phase 2 slope (p2m), phase 2 intercept (p2i), phase 3 slope (p3m), phase 3 intercept (p3i). In addition, standard ventilator settings were recorded

# Volumetric capnography

**Table 1.** Summary of the results

Features	Model	Stage I		Stage II		Stage III		Overall	
		N=867		N=75		N=808		N=1750	
		R <sup>2</sup>	Bias (Mean ± SD)	R <sup>2</sup>	Bias (Mean ± SD)	R <sup>2</sup>	Bias (Mean ± SD)	R <sup>2</sup>	Bias (Mean ± SD)
eTCO <sub>2</sub>	Linear	0.96 <sup>#</sup>	2.91±3.87	0.14 <sup>#</sup>	-8.44±6.45	0.81 <sup>#</sup>	-5.47±7.97	0.83 <sup>#</sup>	-1.45±7.59
eTCO <sub>2</sub>	M5P	0.95 <sup>#</sup>	3.65±4.10	0.13 <sup>*</sup>	-5.98±6.17	0.83 <sup>#</sup>	-3.43±7.46	0.84 <sup>#</sup>	-0.03±7.01
eTCO <sub>2</sub> , IBI, p2m, p3m	Linear	0.96 <sup>#</sup>	-3.97±3.92	0.11 <sup>*</sup>	-4.64±5.83	0.80 <sup>#</sup>	-2.82±7.93	0.85 <sup>#</sup>	0.00±6.94
eTCO <sub>2</sub> , IBI, p2m, p3m	M5P	0.96 <sup>#</sup>	1.89±3.84	0.25 <sup>#</sup>	-1.62±5.06	0.86 <sup>#</sup>	-1.92±6.71	0.90 <sup>#</sup>	-0.01±5.73

<sup>#</sup>P<0.001; <sup>\*</sup>P<0.01.

including respiratory rate, tidal volume, minute volume, FiO<sub>2</sub>, and I:E ratio. The inter-breath interval, IBI, was defined as the time between the start of consecutive breaths measured in seconds. Breath-by-breath Vcap and flow curves were generated by the software and exported as JPEG files for manual review, i.e. to identify artifacts and to assess segmentation quality. For each time point, the last 10 consecutive artifact-free breaths for each ventilator setting were identified and the Vcap parameters calculated and averaged. A composite capnograph overlay image was created to display these last 10 breaths superimposed on each other (**Figure 2**). The IBIs of the 10 breaths at each of the ventilator settings were manually reviewed for each time point and for each animal. Any breaths deviating from the respiratory rate set by the ventilator by > ± 0.02 seconds were automatically excluded. If marked variability was present for at least 4 of the 10 breaths, the time point was discarded.

The following software-derived Vcap variables were used in multivariate analysis to derive estimates of PaCO<sub>2</sub>: eTCO<sub>2</sub>, IBI, p2m, p2i, p3m, p3i, and anatomical dead space. It was determined through model testing that p2i, p3i, and anatomical dead space did not contribute significantly, and these were subsequently dropped from the models. We evaluated 2 models: a standard multivariate linear model and M5P, a well-known machine-learning model. Each of these 2 models encompassed all 3 stages of the experiment; that is, the 2 models were developed using data from all 3 stages, and then were applied to the individual stages.

The M5P model is a regression-tree model [16-18] and is implemented as a part of Weka [19]. It combines an automated classifier which cre-

ates clusters of similar data elements together with an independent least-squares fit for each set of values in the cluster. In our case, the leaves of this tree represent a linear regression of closely related clusters of PaCO<sub>2</sub> test results. The segmentation of clusters was determined automatically by the data heuristics using the M5P algorithm. The resulting model had the advantage of being both transparent to the observer as well as providing an efficient and classical mechanism for prediction through the linear regression component. The resulting model is piecewise linear.

## Statistical analysis

Analysis was performed using R Version 3.02 and the RWeka package [20, 21]. All results are expressed as correlations or means ± SD.

## Results

We analyzed a total of 1750 10-breath sets. Results of fitting the data to the 2 models are shown in **Table 1**. Bland-Altman analysis of the overall data is shown in **Figure 3A-D**. The following equations describe the results of linear regression:

Linear Regression: PaCO<sub>2</sub>=0.8933 \* eTCO<sub>2</sub>+6.2825;

Multiple Linear Regression: PaCO<sub>2</sub>=0.6307 \* eTCO<sub>2</sub>+9.7282 \* p2m+3.0249 \* p3m+1.4702 \* IBI+6.6849.

M5P models for single and multiple variables are provided in the supplemental digital content. Using eTCO<sub>2</sub> alone, PaCO<sub>2</sub> could be accurately estimated in uninjured animals (stage I) with a mean error of 2.91 mmHg (R<sup>2</sup>=0.96, P<0.001) in the linear model, or of 3.65 mmHg (R<sup>2</sup>=0.95, P<0.001) in the M5P model. After

Volumetric capnography

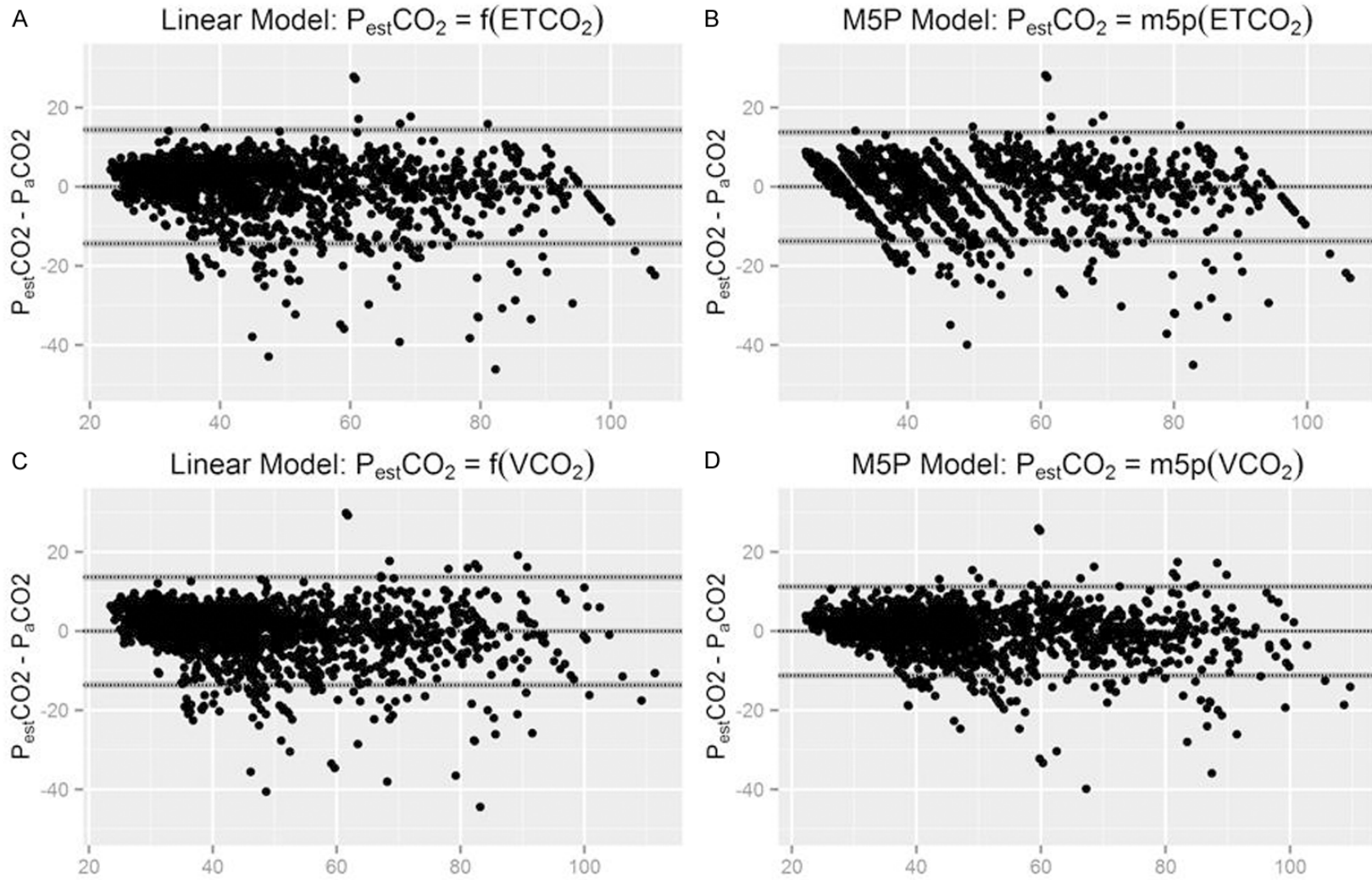


**Figure 3.** Bland-Altman analysis. A:  $\text{eTCO}_2$ -based linear regression model; B:  $\text{eTCO}_2$ -based M5P model; C:  $\text{Vcap}$ -based linear regression model; D:  $\text{Vcap}$ -based M5P model. X axes represent the average of  $\text{PaCO}_2$  and  $P_{\text{EST}}\text{CO}_2$ .

resuscitation (stage III), the mean error for the linear model was -5.47 mmHg ( $R^2=0.81$ ,  $P<0.001$ ) and for the M5P model -3.43 mmHg ( $R^2=0.83$ ). As expected, the relationship deteriorated considerably during the injury/resuscitation stage (stage II), with the mean error for the linear model of -8.44 mmHg ( $R^2=0.14$ ,  $P<0.001$ ) and for M5P of -5.98 mmHg ( $R^2=0.13$ ,  $P<0.01$ ).

By using the additional features of the Vcap curve, all models exhibited improvement in estimation with decreases in the mean error and increases in correlation. Most notable was the improvement in stage II, in which the mean error of the linear model improved to -4.64 mm Hg ( $R^2=0.11$ ,  $P<0.01$ ), and that of the M5P model improved to -1.62 mm Hg ( $R^2=0.25$ ,  $P<0.01$ ). For stages I and III, slight improvements in the average error and correlation were also noted (**Table 1**).

### Discussion

The principal finding of this study is that multivariate analysis of the Vcap waveform improved our ability to estimate PaCO<sub>2</sub> during unstable conditions in a porcine model of chest trauma and resuscitation, compared with the eTCO<sub>2</sub> alone. Having an accurate assessment of PaCO<sub>2</sub> is important in clinical practice, as it could reduce the need for invasive blood gas sampling to verify adequacy of ventilation. This capability is needed for any intubated patient, but is especially important for maintaining normoventilation in patients with traumatic brain injury [4, 22].

Previously, we showed that end-tidal capnography provides an accurate estimate of PaCO<sub>2</sub> under stable hemodynamic and respiratory conditions, but fails during unstable conditions [10, 23]. Several techniques have been described in an effort to improve the non-invasive PaCO<sub>2</sub> estimate. One of them, described by Fletcher [24], involves halving the ventilator respiratory rate and doubling the tidal volume while keeping the inspiratory time constant. The change in eTCO<sub>2</sub> is expected to be proportional to the original PaCO<sub>2</sub>-eTCO<sub>2</sub> difference. However, the actual results were mixed and the maneuver had a variable effect on eTCO<sub>2</sub>, depending on lung function. Another technique for estimation of PaCO<sub>2</sub> from eTCO<sub>2</sub> was described by Tavernier et al. [25]. It involves

prolonged expiration maneuvers. This technique is based on the assumption that a prolonged or forced expiration for 5-15 seconds may provide a better correlation with PaCO<sub>2</sub>. However, end-expiration PCO<sub>2</sub> correlated poorly with PaCO<sub>2</sub>. A recent work by Khemani et al. [26] described application of a multivariate Gaussian process model, which incorporated ventilator-derived data with non-invasive variables such as the eTCO<sub>2</sub> and pulse oximetry to improve estimation of the PaCO<sub>2</sub>. The authors reported that this model predicted PaCO<sub>2</sub> within  $\pm 6$  mmHg of the observed values, 80% of the time.

In the present study, we retrospectively applied multivariate modeling techniques to a set of capnographic waveform data. Morphology of the recorded waveforms was parameterized using a custom-designed Java-based program. The slopes of phases 2 and 3 were retained in this model. These variables provide important information on ventilation-perfusion relationships in the lungs [15, 27, 28]. Fowler (29) proposed that a sloping phase 3 reflected non-uniformity of ventilation. He attributed this in turn to 2 factors. First (the *regional theory*), there is regional non-uniformity of ventilation; inspired gas is distributed unevenly to different zones in the lung. Second (the *sequential theory*), there is temporal non-uniformity of alveolar expansion, such that some areas fill before and empty after other areas. This causes dead space gas to be distributed preferentially to the latter regions [30].

Clinically, Tusman [27] showed that both slope II and slope III were proportional to pulmonary blood flow in patients coming off of cardiopulmonary bypass. Relatedly, slope III is abnormal in patients with pulmonary embolus [31]. Several studies have demonstrated that patients with chronic obstructive lung disease have abnormal Vcap data, which deteriorate with advanced disease [32]. Mechanically ventilated patients with ARDS differ from normal patients on multiple Vcap variables [33].

In the present study, we used a well-characterized model of unilateral pulmonary contusion followed by hemorrhage and aggressive resuscitation, as well as a new model of bilateral pulmonary contusion without additional hemorrhage. We previously used the multiple inert gas elimination technique (MIGET) to establish

that a large increase in true shunt (from 4 to 33%) occurs in the unilateral contusion model. Initially, blood flow increased to low and very low V/Q compartments as well [34]. Thus, our data are consistent with the concept that V/Q mismatch influences the Vcap waveform, and specifically the phase 3 slope, in ARDS [35].

We analyzed our data using multivariate linear regression or a tree-based machine-learning model, which permitted us to calculate  $P_{EST}CO_2$  values solely based on non-invasive capnographic parameters. Unlike the method described by Fletcher, our process did not require any alterations to ventilator parameters, e.g. respiratory rates or tidal volumes [24]. Our approach would be useful for critically ill patients, in whom such changes may be detrimental.

Our study had the following limitations. This analysis was carried out retrospectively using stringent selection criteria for breath quality, as well as manual review of the waveforms. The utility of such method when applied prospectively without human oversight is yet to be proven. In order to improve the quality of data, we completed manual review of the 10-breath datasets for noise and spurious detection prior commencing the final analysis. This resulted in the inclusion of only 75 10-breath sets from stage II (injury/resuscitation). Due to the relatively small size of the set, especially during the acute injury state, we used the entire data set for developing the models and did not use a separate data set for testing [36]. Such approach may have resulted in higher accuracy of  $P_{EST}CO_2$  than would have been achieved otherwise. Finally, the clinical utility of this approach has yet to be proven.

### Conclusions

Porcine models of chest trauma and hemorrhage were used to develop models for predicting  $PaCO_2$  from the exhaled  $PCO_2$ . Multiple features of the Vcap curve, including  $eTCO_2$ , the inter-breath interval, and the slopes of phases 2 and 3 of the curve, were incorporated into a model that improves  $PaCO_2$  estimation over that obtained from the  $eTCO_2$  alone. This model functioned well for subsets of the data from before injury, during injury/resuscitation, and after recovery. This approach merits prospective validation in other models of disease and injury.

### Acknowledgements

The authors wish to thank Kerfoot Walker and Corina Necsoiu, MD for technical support. This research was supported in part by an appointment to the Knowledge Preservation Program at the U.S. Army Institute of Surgical Research administered by the Oak Ridge Institute for Science and Education through an interagency agreement between the U.S. Department of Energy and the U.S. Army Medical Research and Materiel Command. Funded by the Comprehensive Intensive Care Research Task Area of the U.S. Army Medical Research and Materiel Command, Fort Detrick, MD. Note: The opinions or assertions contained herein are the private views of the authors and are not to be construed as official or as reflecting the views of the Department of the Army or the Department of Defense.

### Disclosure of conflict of interest

None.

**Address correspondence to:** Dr. Leopoldo C Cancio, U.S. Army Institute of Surgical Research 3698 Chambers Pass, Fort Sam Houston, TX 78234-6315, USA. Tel: 210-539-6734; E-mail: [divego99@gmail.com](mailto:divego99@gmail.com)

### References

- [1] Walsh BK, Crotwell DN, Restrepo RD. Capnography/capnometry during mechanical ventilation: 2011. *Respir Care* 2011; 56: 503-509.
- [2] Belenkiy SM, Berry JS, Batchinsky AI, Kendrick C, Necsoiu C, Jordan BS, Salinas J, Cancio LC. The noninvasive carbon dioxide gradient (NICO2G) during hemorrhagic shock. *Shock* 2014; 42: 38-43.
- [3] Neumar RW, Otto CW, Link MS, Kronick SL, Shuster M, Callaway CW, Kudenchuk PJ, Ornato JP, McNally B, Silvers SM, Passman RS, White RD, Hess EP, Tang W, Davis D, Sinz E, Morrison LJ. Part 8: adult advanced cardiovascular life support: 2010 American Heart Association Guidelines for Cardiopulmonary Resuscitation and Emergency Cardiovascular Care. *Circulation* 2010; 122 Suppl 3: S729-67.
- [4] Davis DP, Idris AH, Sise MJ, Kennedy F, Eastman AB, Velky T, Vilke GM, Hoyt DB. Early ventilation and outcome in patients with moderate to severe traumatic brain injury. *Crit Care Med* 2006; 34: 1202-8.
- [5] Standards Practice Parameters Committee, American Society of Anesthesiologists. Stan-

## Volumetric capnography

- dards for basic anesthetic monitoring 2011; Available at [www.asahq.org/](http://www.asahq.org/). Accessed 14 June 2015.
- [6] American College of Surgeons Committee on Trauma: Advanced Trauma Life Support Student Course Manual. Chicago, IL: American College of Surgeons 2012.
- [7] Knuth T, Letarte P, Ling G, Moores L, Rhee P, Tauber D and Trask A. Guidelines for the field management of combat-related head trauma. New York: Brain Trauma Foundation; 2005.
- [8] McSwain SD, Hamel DS, Smith PB, Gentile MA, Srinivasan S, Meliones JN, Cheifetz IM. End-tidal and arterial carbon dioxide measurements correlate across all levels of physiologic dead space. *Respir Care* 2010; 55: 288-93.
- [9] Jin X, Weil MH, Tang W, Povoas H, Pernat A, Xie J, Bisera J. End-tidal carbon dioxide as a noninvasive indicator of cardiac index during circulatory shock. *Crit Care Med* 2000; 28: 2415-9.
- [10] Isbell CL, Batchinsky AI, Hetz KM, Baker WL, Cancio LC. Correlation between capnography and arterial carbon dioxide before, during, and after severe chest injury in swine. *Shock* 2012; 37: 103-9.
- [11] Tusman G, Suarez-Sipmann F, Bohm SH, Borges JB, Hedenstierna G. Hedenstierna: Capnography reflects ventilation/perfusion distribution in a model of acute lung injury. *Acta Anaesthesiol Scand* 2011; 55: 597-606.
- [12] Patel MM, Rayburn DB, Browning JA, Kline JA. Neural network analysis of the volumetric capnogram to detect pulmonary embolism. *Chest* 1999; 116: 1325-1332.
- [13] Batchinsky AI, Jordan BS, Necsoiu C, Dubick MA, Cancio LC. Cancio: Dynamic changes in shunt and ventilation-perfusion mismatch following experimental pulmonary contusion. *Shock* 2010; 33: 419-25.
- [14] Fletcher R, Jonson B. Prediction of the physiological dead space/tidal volume ratio during anaesthesia/IPPV from simple pre-operative tests. *Acta Anaesthesiol Scand* 1981; 25: 58-62.
- [15] Fletcher R, Jonson B, Cumming G, Brew J. The concept of deadspace with special reference to the single breath test for carbon dioxide. *Br J Anaesth* 1981; 53: 77-88.
- [16] Torgo L. Inductive learning of tree-based regression models. *AI Communications* 2000; 13: 137-138. Available at <http://www.ncc.up.pt/~ltorgo/PhD/>. Accessed 14 June 2015.
- [17] Quinlan JR. Learning with continuous classes. 5th Australian Joint Conference on Artificial Intelligence. Vol. 92. Singapore 1992; pp. 343-348.
- [18] Wang Y and Witten IH. Induction of model trees for predicting continuous classes. Working paper 96/23. Available at <http://www.cs.waikato.ac.nz/pubs/wp/1996/uow-cs-wp-1996-23.pdf>. Accessed 14 June 2015. Department of Computer Science, The University of Waikato, Hamilton, New Zealand; 1996.
- [19] Hall M, Frank E, Holmes G, Pfahringer B, Reutemann P and Witten IH. The WEKA data mining software: an update. Available at [http://www.cms.waikato.ac.nz/~ml/publications/2009/weka\\_update.pdf](http://www.cms.waikato.ac.nz/~ml/publications/2009/weka_update.pdf). Accessed 14 June 2015. *SIGKDD Explorations* 2009; 11: 10-18.
- [20] R Development Core Team: R: A Language and Environment for Statistical Computing. Available at <http://www.R-project.org>. Accessed 14 June 2015.
- [21] Hornik K, Buchta C and Zeileis A. Open-source machine learning: R meets Weka. *Computational Statistics* 2009; 24: 225-232.
- [22] Cancio LC and Chung KK. The role of normoventilation in improving traumatic brain injury outcomes. *US Army Med Depart J* 2011; 49-54.
- [23] Belenkiy S, Ivey KM, Batchinsky AI, Langer T, Necsoiu C, Baker W, Salinas J, Cancio LC. Noninvasive carbon dioxide monitoring in a porcine model of acute lung injury due to smoke inhalation and burns. *Shock* 2013; 39: 495-500.
- [24] Fletcher R and Boris-Möller F. Can we improve the estimate of arterial PCO<sub>2</sub> from end-tidal PCO<sub>2</sub>? *Europ J Anaesthesiol* 2000; 17: 306-310.
- [25] Tavernier B, Rey D, Thevenin D, Triboulet J and Scherpereel P. Can prolonged expiration manoeuvres improve the prediction of arterial PCO<sub>2</sub> from end-tidal PCO<sub>2</sub>? *Br J Anaesth* 1997; 78: 536-540.
- [26] Khemani RG, Celikkaya EB, Shelton CR, Kale D, Ross PA, Wetzel RC and Newth CJ. Algorithms to estimate PaCO<sub>2</sub> and pH using noninvasive parameters for children with hypoxemic respiratory failure. *Respir Care* 2014; 59: 1248-57.
- [27] Tusman G, Areta M, Climente C, Plit R, Suarez-Sipmann F, Rodríguez-Nieto MJ, Peces-Barba G, Turchetto E, Böhm SH. Effect of pulmonary perfusion on the slopes of single-breath test of CO<sub>2</sub>. *J Appl Physiol* 2005; 99: 650-655.
- [28] Tusman G, Sipmann FS and Bohm SH. Rationale of dead space measurement by volumetric capnography. *Anesth Analg* 2012; 114: 866-874.
- [29] Fowler WS. Lung function studies. III. Uneven pulmonary ventilation in normal subjects and in patients with pulmonary disease. *J Appl Physiol* 1949; 2: 283-299.
- [30] Klocke RA. Dead space: Simplicity to complexity. *J Appl Physiol* 2006; 100: 1-2.
- [31] Verschuren F, Liistro G, Coffeng R, Thys F, Roeseler J, Zech F and Reynaert M. Volumetric



## Volumetric capnography

- capnography as a screening test for pulmonary embolism in the emergency department. *Chest* 2004; 125: 841-850.
- [32] Romero PV, Rodriguez B, de Oliveira D, Blanch L and Manresa F. Volumetric capnography and chronic obstructive pulmonary disease staging. *Int J Chron Obstruct Pulmon Dis* 2007; 2: 381-91.
- [33] Romero PV, Lucangelo U, Lopez Aguilar J, Fernandez R and Blanch L. Physiologically based indices of volumetric capnography in patients receiving mechanical ventilation. *Eur Respir J* 1997; 10: 1309-15.
- [34] Batchinsky AI, Jordan BS, Necsoiu C, Dubick MA and Cancio LC. Dynamic changes in shunt and ventilation-perfusion mismatch following experimental pulmonary contusion. *Shock* 2010; 33: 419-425.
- [35] Tusman G, Suarez-Sipmann F, Bohm SH, Borges JB and Hedenstierna G. Capnography reflects ventilation/perfusion distribution in a model of acute lung injury. *Acta Anaes Scand* 2011; 55: 597-606.
- [36] Dobbin KK and Simon RM. Optimally splitting cases for training and testing high dimensional classifiers. *BMC Med Genom* 2011; 4: 31.